Cell Tissue Res (2005) 320: 33–50
DOI 10.1007/s00441-004-1054-8

REGULAR ARTICLE

Peter Blaesse · Sascha Ehrhardt · Eckhard Friauf · Hans Gerd Nothwang

Developmental pattern of three vesicular glutamate transporters in the rat superior olivary complex

Received: 12 November 2004 / Accepted: 15 November 2004 / Published online: 16 February 2005

Abstract Vesicular glutamate transporters (VGLUTs) mediate the packaging of the excitatory neurotransmitter glutamate into synaptic vesicles. Three VGLUT subtypes have been identified so far, which are differentially expressed in the brain. Here, we have investigated the spatiotemporal distribution of the three VGLUTs in the rat superior olivary complex (SOC), a prominent processing center, which receives strong glutamatergic inputs and which lies within the auditory brainstem. Immunoreactivity (ir) against all three VGLUTs was found in the SOC nuclei throughout development (postnatal days P0–P60). It was predominantly seen in axon terminals, although cytoplasmic labeling also occurred. Each transporter displayed a characteristic expression pattern. In the adult SOC, VGLUT1 labeling varied from strong in the medial nucleus of the trapezoid body, lateral superior olive, and medial superior olive (MSO) to moderate (ventral and lateral nuclei of the trapezoid body) to faint (superior paraolivary nucleus). VGLUT2-ir was moderate to strong throughout the SOC, whereas VGLUT3 was only weakly expressed. These results extend previous reports on co-localization of VGLUTs in the auditory brainstem. As in the adult, specific features were seen during development for all three transporters. Intensity increases and decreases occurred with both VGLUT1 and VGLUT3, whereas VGLUT2-ir remained moderately high throughout development. A striking result was obtained with VGLUT3, which was only transiently expressed in the different SOC nuclei between P0 and P12. A transient occurrence of VGLUT1-immunoreactive terminals on somata of MSO neurons was another striking finding. Our results imply a considerable amount of synaptic reorganization in the glutamatergic inputs to the SOC and suggest differential roles of VGLUTs during maturation and in adulthood.

Keywords VGLUT · Brain development · Auditory brainstem · Superior olivary complex · Immunohistochemistry · Rat (Sprague Dawley)

This work was supported by the Graduate Research School "Molecular, physiological and pharmacological analysis of cellular membrane transport", DFG GRK 845/1.

P. Blaesse · S. Ehrhardt · E. Friauf · H. G. Nothwang (✉)
Abteilung Tierphysiologie, Fachbereich Biologie,
Technische Universität Kaiserslautern,
Kaiserslautern, Deutschland
e-mail: nothwang@rhrk.uni-kl.de
Tel.: +49-631-205-4669
Fax: +49-631-205-4684

Introduction

Glutamate is the major excitatory neurotransmitter in the mammalian central nervous system. Prior to their exocytic release, neurotransmitter molecules must be sequestered into synaptic vesicles. The uptake process is H^+-dependent and, in the case of glutamate, is mediated by vesicular glutamate transporters (VGLUTs), of which three have been identified and characterized so far. VGLUT1 was originally isolated as a brain-specific Na^+-dependent plasma-membrane carrier for inorganic phosphate (BNPI; Ni et al. 1994); however, subsequent analysis has shown it to be a vesicular glutamate transporter (Bellocchio et al. 2000; Takamori et al. 2000). VGLUT2 (originally differentiation-associated brain-specific phosphate transporter; Aihara et al. 2000) and VGLUT3 were identified as vesicular glutamate transporters from their sequence homology to VGLUT1 (Fremeau et al. 2001, 2002; Herzog et al. 2001; Takamori et al. 2001, 2002; Gras et al. 2002; Schäfer et al. 2002; Varoqui et al. 2002). The expression of VGLUT1 and VGLUT2 is restricted to the brain, whereas VGLUT3 is also expressed in liver and kidney (Fremeau et al. 2002; Gras et al. 2002). All three transporters are highly homologous (>70% amino acid identity) and accumulate L-glutamate with similar bioenergetic and pharmacological characteristics (Fremeau et al. 2002; Gras et al. 2002; Takamori et al. 2002).

Within the brain, the regional distribution of the expression of the various VGLUT forms from the VGLUT gene differs from one another (for reviews, see Hisano 2003; Fremeau et al. 2004b). VGLUT1 and VGLUT2 show a widespread, albeit discrete and strikingly complementary

distribution. VGLUT1 expression is strong in the cerebral and cerebellar cortices, the olfactory bulb, and the hippocampus, whereas VGLUT2 is predominantly expressed in the thalamus, brainstem, and deep cerebellar nuclei (Ni et al. 1995; Fremeau et al. 2001; Herzog et al. 2001; Varoqui et al. 2002). Within the cerebellum, the two types of excitatory input onto Purkinje cells display a complementary pattern in that VGLUT1 is expressed in the parallel fibers, whereas VGLUT2 is expressed in the climbing fibers (Miyazaki et al. 2003). Recently, complementary expression has also been reported in the retina (Fyk-Kolodziej et al. 2004). In contrast to the widespread distribution of VGLUT1 and VGLUT2, VGLUT3 expression in the brain is restricted to discrete cell populations scattered in the striatum, hippocampus, cerebral cortex, raphe nuclei, hypothalamic nuclei, and brainstem (Fremeau et al. 2002; Gras et al. 2002; Schäfer et al. 2002; Herzog et al. 2004). Furthermore, VGLUT3 is not found in conventional glutamatergic neurons, but in neurons known to release other transmitter molecules, such as acetylcholine, serotonin, gamma aminobutyric acid (GABA), and glycine (Fremeau et al. 2002; Gras et al. 2002; Schäfer et al. 2002; Haverkamp and Wässle 2004). This suggests an unsuspected function of VGLUT3 in subsets of interneurons and in neuromodulatory neurons (Herzog et al. 2004).

The expression of these transporters is age-dependent: VGLUT1 is up-regulated with age (Ni et al. 1995; Schäfer et al. 2002; Miyazaki et al. 2003), whereas VGLUT2 is down-regulated (Miyazaki et al. 2003). Furthermore, subtype switching from the VGLUT2 to the VGLUT1 isoform occurs in the developing mouse cerebellum in synapses between parallel fibers and Purkinje cells (Miyazaki et al. 2003). To our knowledge, VGLUT3 development has not been analyzed thus far in the brain.

In the mammalian central auditory system, temporal precision is of crucial importance for processing acoustic information, such as the computing of interaural time differences and intensity differences to localize sound sources (Yin 2002). The fast excitatory neurotransmission in the auditory brainstem is mediated by glutamatergic synapses, and these synapses display high-fidelity neurotransmission and transmit signals at a high frequency rate. To this end, specializations exist at both the morphological and the molecular level. A morphological example is provided by the calyces of Held in the superior olivary complex (SOC); these faithfully transmit signals with frequencies of up to 600 Hz (Wu and Kelly 1993). At the molecular level, AMPA and kainate receptors, known to mediate rapid glutamatergic transmission (for a review, see Dingledine et al. 1999) with desensitization time constants of about 1 ms (Raman et al. 1994), are notable examples (Oertel and Wickesberg 1993; Caicedo and Eybalin 1999; Löhrke and Friauf 2002; Vitten et al. 2004). Another example is provided by various K^+ channels that limit the duration of action potentials and thus regulate action potential firing (Brew and Forsythe 1995; Trussell 1999; Dodson and Forsythe 2004). Similar specializations may occur in the distribution of VGLUTs in neurons with high-fidelity neurotransmission. Thus far, VGLUT expression in auditory brainstem nuclei has not been investigated in-depth. From existing studies, moderate levels of VGLUT1 protein are known to be present in the adult rat inferior colliculus (Herzog et al. 2001; Kaneko et al. 2002) and in the SOC (Kaneko et al. 2002; Varoqui et al. 2002), whereas stronger expression is observed in the cochlear nuclear complex (Kaneko et al. 2002). High levels of VGLUT2 protein have been described in the inferior colliculus (Herzog et al. 2001; Kaneko et al. 2002) and moderate levels in the SOC and the cochlear nuclear complex (Kaneko et al. 2002; Varoqui et al. 2002). Data on VGLUT3 expression in the auditory brainstem are rare; a faint immunoreactive signal has been seen in the adult rat inferior colliculus (Gras et al. 2002).

We have studied the expression of all three VGLUT isoforms in the rat SOC, a prominent processing center in the mammalian auditory brainstem (for a review, see Schwartz 1992). At present, little information is available regarding VGLUT distribution in the individual SOC nuclei. Our study has differentiated between six SOC nuclei: the lateral superior olive (LSO), the medial superior olive (MSO), the medial nucleus of the trapezoid body (MNTB), the superior paraolivary nucleus (SPN), the ventral nucleus of the trapezoid body (VNTB), and the lateral nucleus of the trapezoid body (LNTB). In order to assess the distribution of the VGLUT isoforms at the cellular level, we have employed immunohistochemistry and confocal microscopy. The distribution has been analyzed both in adulthood and during early postnatal development, comprising a total of four different ages. We have particularly addressed the question of whether nucleus-specific expression patterns are present in the SOC. Our results show that all three VGLUT isoforms are present in the SOC nuclei, both during early postnatal development and in adulthood. The immunofluorescent pattern of VGLUTs, however, differs across the various nuclei and display developmental changes both in intensity and distribution.

Materials and methods

The experiments were performed on 20 Sprague–Dawley rats of both genders, aged between postnatal day 0 (P0, i.e., the day of birth) and P60. Animals were bred and housed in our animal facility and treated in compliance with the current German Animal Protection Law. All protocols were approved by the regional animal care and use committee (Landesuntersuchungsamt Koblenz, Germany) and adhered to the NIH Guide for the Care and Use of Laboratory Animals.

Animals were deeply anesthetized with chloral hydrate (700 mg kg^{-1} body weight i.p.) and perfused transcardially with 0.01 M phosphate-buffered saline (PBS, pH 7.4), followed by Zamboni's solution (2% paraformaldehyde, 15% picric acid in 0.1 M phosphate buffer). Brains were removed and stored in fixative overnight at 7°C. After incubation in 30% sucrose/PBS for cryoprotection, 30-μm-thick coronal sections were cut through the brainstem, collected in 15% sucrose/PBS, thoroughly rinsed in PBS, and blocked for 1 h in 3% bovine serum albumin (BSA),

10% goat serum, and 0.3% Triton in TRIS-buffered saline (pH 7.4). The primary antisera (rabbit anti-VGLUT1, rabbit anti-VGLUT2, rabbit anti-VGLUT3) were a generous gift by Dr. S. El Mestikawy (Creteil, Cedex, France) and have been characterized previously (VGLUT1 and VGLUT2: Herzog et al. 2001; VGLUT3: Gras et al. 2002). The primary mouse anti-MAP2 antiserum was obtained from Sigma (Germany) and used to counterstain the sections in order to reveal neuronal somata and neuropil. Antibodies were diluted either 1:500 (anti-VGLUT1, anti-VGLUT2, and anti-MAP2) or 1:1,000 (anti-VGLUT3) and added to the blocking solution. Incubation with agitation was carried out at 7°C for 24 h. After several rinses in PBS, sections were transferred to carrier solution (0.3% Triton, 1% BSA, 1% goat serum) and treated with the secondary antibodies, viz., goat anti-rabbit conjugated to Alexa Fluor 488 and goat anti-mouse conjugated to Alexa Fluor 546 (both diluted 1:1,000; Molecular Probes, The Netherlands). Sections were incubated overnight at 7°C, rinsed again, mounted on slides, and air-dried. Coverslips were mounted with Vectashield H-1400 anti-fade mounting medium (Vector laboratories, Canada). Control experiments were performed by omission of either the VGLUT antibodies or secondary antibodies and resulted in the absence of VGLUT immunosignal. Images were taken on a confocal laser scanning microscope (Zeiss LSM 510; Zeiss, Germany) equipped with argon (488 nm) and helium–neon (543 nm) lasers and appropriate excitation and emission filters for the maximum separation of Alexa Fluor 488 (488 nm excitation, filter BP 505–550) and Alexa Fluor 546 (543 nm excitation, filter LP 560). The configuration used was confirmed to prevent bleed-through. A 10× objective lens (Plan-Neofluar 10×/0.3; Zeiss) and a 40× oil immersion objective lens (Plan-Neofluar 40×/1.3 oil; Zeiss) were used. A pinhole size of 67 μm resulted in optical sections of <10 μm thickness for the 10× objective lens and <1 μm for the 40× objective lens. Images of 2048×2048 pixels were obtained and further processed with Zeiss LSM Image browser software 2.80. Figures were prepared on a PC running Adobe Photoshop 5.5 (Adobe systems, San Francisco, Calif.).

Results

VGLUT immunoreactivity in the adult SOC

In the SOC of adult rats (Figs. 1, 2), every nucleus of the six SOC nuclei analyzed (MNTB, VNTB, LNTB, LSO, MSO, and SPN) contained each transporter isoform. However, both the labeling intensity and the cellular distribution patterns differed among the nuclei. For each transporter, unique patterns were revealed. Therefore, each transporter will be described separately: first VGLUT1, then VGLUT2, and finally VGLUT3. A summary of the results is given in Table 1.

VGLUT1 immunoreactivity in the adult SOC

Strong VGLUT1 immunoreactivity (VGLUT1-ir) was observed in the MNTB, the LSO, and the MSO. The VNTB and LNTB contained moderate immunoreactivity, and the SPN was weakly labeled (Figs. 1, 2). No staining was visible in the areas surrounding the SOC, consistent with previous analysis (Kaneko et al. 2002; Varoqui et al. 2002). Analysis at higher magnification demonstrated a specific distribution of VGLUT1-ir across the various nuclei. In the MNTB, the signal was restricted to the calyces of Held, displaying a thick and fenestrated labeling pattern around the somata of almost all MNTB principal neurons (Fig. 1a). In contrast, only some somata of VNTB neurons were covered by labeled structures, presumably representing axonal synaptic terminals (Fig. 1b). In the LNTB, many (but not all) somata were surrounded by immunoreactive puncta, displaying a disc-shaped pattern (Fig. 1c). The perisomatic labeling pattern observed in the MNTB, the VNTB, and the LNTB was not present in the other three SOC nuclei. Instead, punctate VGLUT1-ir occurred in the neuropil of the LSO, the MSO, and the SPN (Fig. 2a–c). In the latter nucleus, only a few immunopositive puncta were observed (Fig. 2c).

VGLUT2 immunoreactivity in the adult SOC

VGLUT2-ir was prominent throughout the SOC, as all nuclei displayed moderate to strong signal intensities, with the VNTB being most heavily labeled (Figs. 1, 2). The surrounding brainstem areas were also labeled, and we found no unlabeled areas in our sections (data not shown) consistent with the known widespread distribution of VGLUT2 in the brainstem (Fremeau et al. 2001; Varoqui et al. 2002; Kaneko et al. 2002). In the MNTB, VGLUT2-ir was similar to that obtained with VGLUT1 regarding the labeling of the calyces of Held (Fig. 1d). However, immunoreactive grains also occurred in the neuropil. In the VNTB, a punctate labeling pattern was seen around the somata and in the neuropil (Fig. 1e). An unusual form of perisomatic VGLUT2-ir occurred in the LNTB, where we found disc-shaped signals on the majority of neurons (Fig. 1f). In the LSO, VGLUT2-ir had both a grainy and punctate pattern; both signals occurred predominantly in the neuropil (Fig. 2d). Furthermore, LSO somata showed cytoplasmic labeling, a feature that was not observed for the other two transporter isoforms in this nucleus. The MSO showed only a few immunoreactive puncta, which were located in the neuropil (Fig. 2e). In the SPN, the neuropil was also labeled by puncta, and the cytoplasm of many neurons contained labeling (Fig. 2f).

VGLUT3 immunoreactivity in the adult SOC

VGLUT3 showed the weakest immunoreactive signal of the three transporters in the adult SOC. All nuclei were

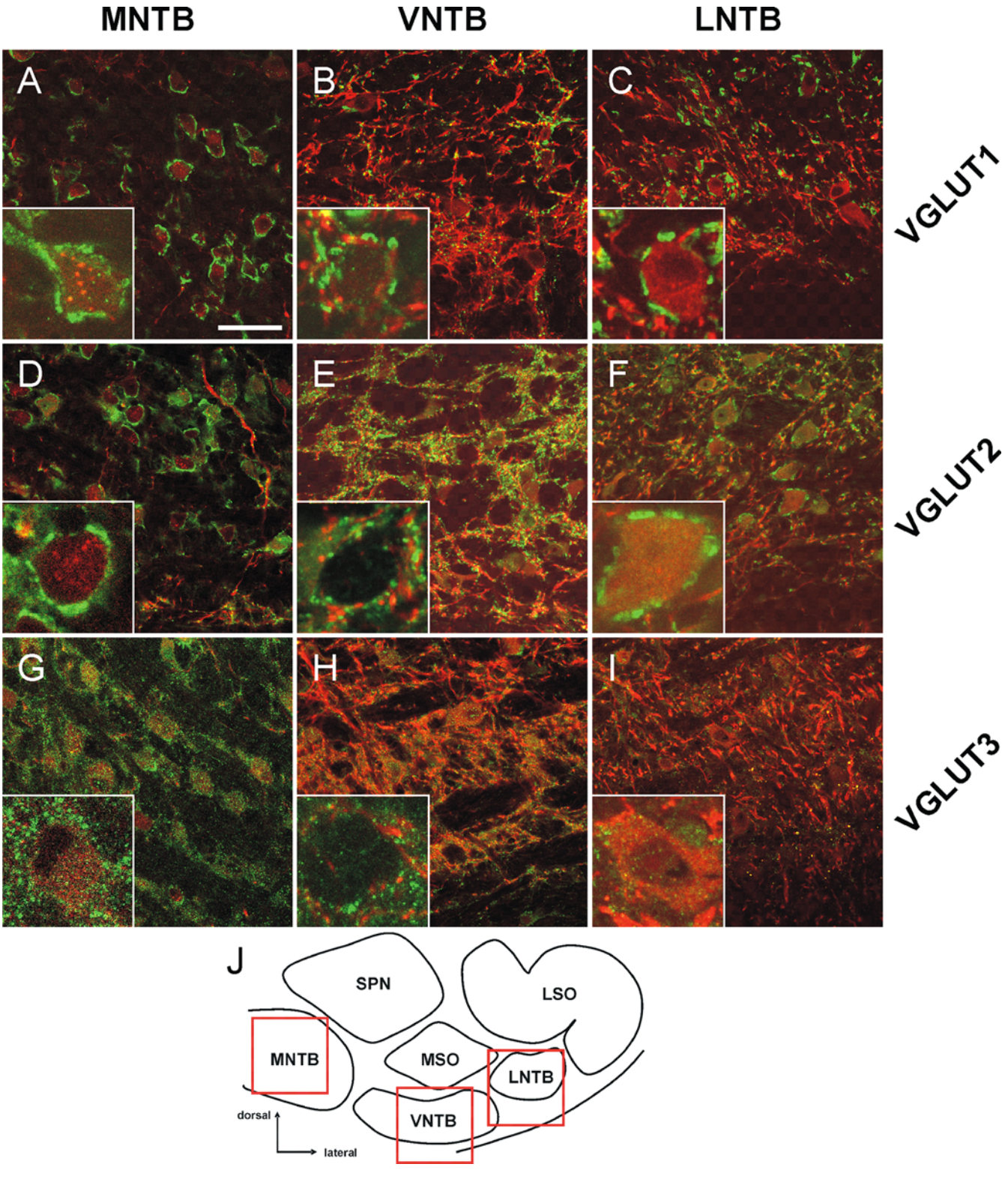

labeled, but the SPN signal was only barely visible (Figs. 1, 2). In the MNTB, the characteristic labeling pattern observed with VGLUT1 and VGLUT2, namely the outline of the calyces of Held, was not revealed by VGLUT3-ir (Fig. 1g). Instead, the immunoreactive signals were grainy and diffusely spread over the cell surfaces and in the cytoplasm; no grains were found in the fascicles formed by axons of the trapezoid body. The staining patterns in the other five SOC nuclei were similar to each other in that labeling was weak, diffuse, and grainy; perisomatic distributions were rare (Figs. 1h, i, 2g–i).

◀ **Fig. 1** **a–i** High magnification confocal images illustrating VGLUT immunoreactivity (VGLUT-ir) in the MNTB, VNTB, and LNTB of adult rats (P60). VGLUT-ir is *green*, and MAP2-ir is *red*. **a** In the MNTB, VGLUT1-ir is strong and restricted to the calyces of Held. Note the thick and fenestrated labeling pattern around the somata of MNTB principal neurons (*inset*). Almost every MNTB principal neuron appears to be decorated. **b** In the VNTB, moderate VGLUT1-ir occurs in a diffuse pattern. A few somata are covered by puncta (*inset*). **c** In the LNTB, VGLUT1-ir puncta occur in the neuropil and on somata, where they are dense, sometimes merging into flat discs (*inset*). **d** In the MNTB, VGLUT2-ir around somata resembles that of VGLUT1 in terms of intensity, thickness, and fenestrated pattern (*inset*). In addition, immunoreactive grains occur in the neuropil. **e** In the VNTB, VGLUT2-ir is strong, and puncta are present around the somata (*inset*) and in the neuropil. **f** In the LNTB, VGLUT2-ir is also present around somata and in the neuropil. In contrast to the labeling pattern in the MNTB (**d**) and VNTB (**e**), the perisomatic immunoreactivity has a disc-shaped pattern (*inset*). A faint signal appears to be present in the cytoplasm of LNTB neurons. **g** In the MNTB, the pattern of VGLUT3-ir differs from that obtained with VGLUT1 and VGLUT2, being grainy and diffuse. Immunoreactive grains also appear in the cytoplasm (*inset*). **h** In the VNTB, VGLUT3-ir has a grainy and diffuse pattern and occurs mainly in the neuropil (*inset*). **i** In the LNTB, VGLUT3-ir is similar to that seen in the VNTB. **j** Semi-schematic representation of the rat SOC, illustrating the six nuclei (*red squares* localization of the high power photomicrographs). *Bar* 50 μm (*insets* 12.5 μm)

VGLUT immunoreactivity in the developing SOC

To study the spatiotemporal pattern of the three vesicular glutamate transporters during early postnatal development, we analyzed their immunoreactivity at P0, P4, and P12. At all developmental stages, the three transporters were identified in the SOC by immunofluorescence (Fig. 3). As in the adult animals, the immunosignals of the three transporter isoforms differed from each other and will therefore be described separately. A summary of the results is given in Table 1.

VGLUT1 immunoreactivity in the developing SOC

At the day of birth, VGLUT1-ir was most prominent in the LSO and the MSO (Fig. 3a). The MNTB and the LNTB were also clearly labeled at this age. A weak signal was detected in the SPN, and the VNTB was almost unlabeled. With increasing age, the LSO and the MSO remained strongly labeled, whereas the signal intensity increased in the MNTB and the LNTB (Fig. 3b, c). The SPN and the VNTB also showed some increase in labeling intensity, but they remained weakly labeled until P12. At P12, the overall situation seen at low magnification was indistinguishable from that present at P60 (Fig. 3c). Analysis at higher magnification demonstrated that labeling in the MNTB turned from a diffuse and punctate pattern at P0 to an adult-like staining of the calyces of Held at P12 (Fig. 4a–c). At P0 and P4, the VNTB was only weakly (if at all) VGLUT1-immunoreactive (Fig. 5a, b). Labeling intensity increased little thereafter, and at P12, a moderate labeling was present as seen at P60 (Figs. 1b, 5c). In the LNTB, VGLUT1-ir was low at birth and increased until P4, when the adult-like pattern became obvious (Fig. 6a–c). In the developing LSO, perisomatic labeling was prominent at all ages with strong labeling also appearing in the neuropil (Fig. 7a–c). The perisomatic labeling contrasted with that seen at P60, at which stage VGLUT1-ir was restricted to the neuropil (cf. Fig. 2a). The labeling pattern in the MSO was striking as the dendritic regions medial and lateral to the dorso-ventrally oriented somata column were robustly stained between P0 and P12, giving the MSO a rhomboid/diamond-shaped appearance (Fig. 8a–c; see also Fig. 3a–c). At the cellular level, we observed a difference in the labeling pattern between P12 and earlier ages: perisomatic puncta were not present at P0 and P4 (insets in Fig. 8a–c). Interestingly, the perisomatic labeling of MSO neurons disappeared until P60 (cf. Fig. 2b). As mentioned above, VGLUT1-ir in the SPN was weak between P0 and P12 and restricted to a few immunoreactive puncta in the neuropil (Fig. 9a–c). This pattern remained into adulthood.

VGLUT2 immunoreactivity in the developing SOC

At P0, VGLUT2-ir was widespread in the SOC (Fig. 3d). All six nuclei showed immunosignals that remained at older ages (Fig. 3d–f). In the MNTB, high magnification analysis showed a similar change in immunoreactivity as observed for VGLUT1-ir, i.e., from a punctate pattern at P0 to a calyx-shaped pattern at P12 (Fig. 4d–f). Compared with VGLUT1, however, this change appeared to be lagging behind, because the calyx-shaped appearance did not occur in all neurons at P12 (Fig. 4c, f). In the VNTB, a dense punctate labeling pattern occurred in the neuropil and around somata with no considerable changes in intensity (Fig. 5d–f). Even at the youngest age, this pattern was indistinguishable from that of the adult (cf. Fig. 1e). In general, the development of VGLUT2-ir in the LNTB (Fig. 6d–f), LSO (Fig. 7d–f), MSO (Fig. 8d–f), and SPN (Fig. 9d–f) was similar to that seen in the VNTB. However, in the LNTB, the disc-shaped pattern at P60 (cf. Fig. 1f) did not become prominent at P12, indicating that dynamic changes occurred after P12. Furthermore, we observed cytoplasmic labeling in the LSO and MSO at P12 (insets in Figs. 7f, 8f). In contrast to VGLUT1 and VGLUT3, strong staining was also observed in the surrounding regions of the SOC.

VGLUT3 immunoreactivity in the developing SOC

Like the other two transporter isoforms, VGLUT3 was identified immunohistochemically in the SOC as early as the neonatal stages (Fig. 3g–i). A peculiar situation occurred in the MNTB in which a strong cytoplasmic signal was observed in the neuronal somata at P0 and P4, but not at P12 and thereafter (Fig. 4g–i). The calyces of Held, which were immunoreactive for VGLUT1 and VGLUT2, were not labeled by VGLUT3 antiserum. In the VNTB, the labeling changed from a virtual absence of VGLUT3-ir at P0 and P4 into the adult-like pattern with weak, diffuse, grainy signals at P12 (Fig. 5g–i). LNTB neurons displayed a transient labeling pattern in that many puncta were im-

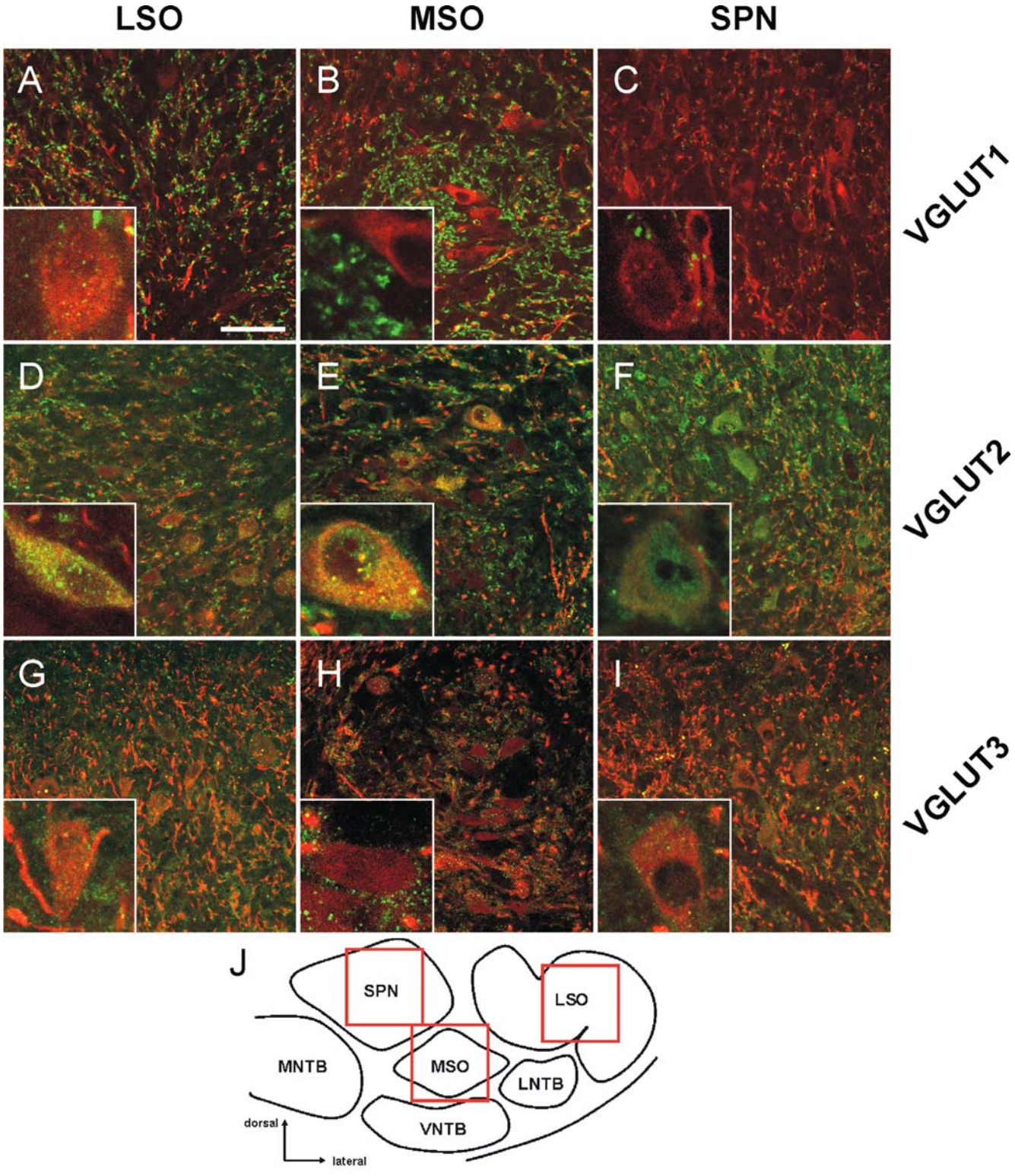

Fig. 2 **a–i** High magnification confocal images illustrating VGLUT-ir in the LSO, MSO, and SPN of adult rats (P60). VGLUT-ir is *green*, and MAP2-ir is *red*. **a** In the LSO, VGLUT1-ir is strong, occurring in a punctate pattern. Puncta are present in the neuropil rather than around the somata (*inset*). **b** In the MSO, VGLUT1-ir is also strong and punctate. As in the LSO, the puncta occur in the neuropil; somata and proximal dendrites appear to be unlabeled (*inset*). **c** In the SPN, only a few VGLUT1-ir puncta can be seen. They occur at the dendrites rather than at the somata (*inset*). **d** In the LSO, VGLUT2-ir has both a grainy and punctate pattern. In addition, cytoplasmic immunoreactivity can be seen (*inset*). **e** In the MSO, VGLUT2-ir is moderate in the neuropil and faint in the cytoplasm; somata are unlabeled (*inset*). **f** In the SPN, VGLUT2-ir is punctate and cytoplasmic labeling occurs in many cells (*inset*). The number of puncta is low. **g** In the LSO, VGLUT3-ir is low and diffuse and has a grainy pattern. The labeling occurs in the neuropil (*inset*). **h** In the MSO, VGLUT3-ir is also low, diffuse, and grainy. In contrast to VGLUT1-ir and VGLUT2-ir (**b, e**), VGLUT3-ir grains are also perisomatic in the MSO (*inset*). **i** In the SPN, a small number of VGLUT3-ir grains is present. These grains are located in the neuropil rather than around the somata (*inset*). **j** Semi-schematic representation of the rat SOC, illustrating the six nuclei (*red squares* localization of the high power photomicrographs). *Bar* 50 μm (*insets* 12.5 μm)

Table 1 Distribution and relative abundance of the three vesicular glutamate transporters, VGLUT1, VGLUT2, and VGLUT3, in the SOC. The relative levels of immunoreactivity are based on visual inspection (− virtually absent, + faint to weak, ++ moderate, +++ strong)

	VGLUT1				VGLUT2				VGLUT3			
	P0	P4	P12	P60	P0	P4	P12	P60	P0	P4	P12	P60
MNTB												
Cytoplasm	−	−	−	−	−	−	−	−	+++	+++	+	+
Perisomatic	+	++	+++	+++	+	++	++	+++	−	−	−	+
Neuropil	++	++	−	−	++	++	+	+	+	+	+	+
VNTB												
Cytoplasm	−	−	−	−	−	−	−	−	−	−	−	−
Perisomatic	−	−	++	++	++	++	++	++	−	−	−	+
Neuropil	−	−	+	+	++	++	++	+++	−	−	+	+
LNTB												
Cytoplasm	−	−	−	−	−	−	−	+	−	−	−	−
Perisomatic	−	++	++	++	++	++	++	++	+	++	−	−
Neuropil	+	++	++	+	++	++	++	++	+	++	+	+
LSO												
Cytoplasm	−	−	−	−	−	−	++	++	−	−	−	−
Perisomatic	++	++	++	−	++	++	++	−	++	++	+++	−
Neuropil	++	++	++	+++	++	++	++	++	+	+	+	+
MSO												
Cytoplasm	−	−	−	−	−	−	++	+	−	−	−	−
Perisomatic	−	−	++	−	+	+	+	−	−	−	++	+
Neuropil	+++	+++	+++	+++	++	++	++	++	−	−	++	+
SPN												
Cytoplasm	−	−	−	−	−	−	−	++	−	−	−	−
Perisomatic	−	−	−	−	++	+	+	−	++	++	+++	−
Neuropil	+	+	+	+	++	++	++	++	++	++	++	+

munoreactive at P0 and P4, whereas by P12, the number of puncta had declined considerably (Fig. 6g–i). Another transient expression became apparent in the LSO. Here, VGLUT3-ir was perisomatic during early postnatal development (Fig. 7g–i), with a high density of puncta at P12, outlining the cell bodies and proximal dendrites (Fig. 7i). This pattern was strikingly different from that seen at P60 (cf. Fig. 2g). As in the VNTB, VGLUT3-ir in the MSO was virtually absent at P0 and P4, becoming prominent at P12, at which time puncta were found around the somata and in the neuropil (Fig. 8g–i). Their number declined thereafter (cf. Fig. 2h). In the SPN, labeling was intense from P0-P12, outlining somata and proximal dendrites at P4 and P12; the neuropil was also stained (Fig. 9g–i). A regressive development took place after P12 in the SPN, since only a small number of VGLUT3-ir puncta remained until adulthood (cf. Fig. 2i).

Discussion

We have examined the spatiotemporal distribution of VGLUT-ir in the rat SOC between birth and 2 months of age and have compared the labeling pattern across six SOC nuclei (cf. Table 1). The main results of our study are: (1) all three VGLUTs are present in the adult SOC, and every isoform is present in each nucleus; (2) each transporter displays a characteristic and unique expression level and cellular labeling pattern; (3) all three VGLUTs are present in the neonatal SOC and thereafter, although several age-related changes occur, including changes in intensity and cellular location. Our results demonstrate considerable differences in the spatiotemporal distribution of the VGLUTs and suggest differential roles during maturation and in adulthood.

Presence of all three VGLUTs in the adult SOC

Our analysis has demonstrated immunofluorescent signals for all three VGLUT isoforms in each nucleus in the adult SOC. This confirms and extends previous findings that have demonstrated the presence of VGLUT1- and VGLUT2-ir in the adult SOC (Kaneko et al. 2002; Varoqui et al. 2002). The co-existence of VGLUTs in individual SOC nuclei is in contrast to many studies that have demonstrated complementary expression of VGLUT1 and VGLUT2 (Ni et al. 1994; Hisano et al. 2000; Fremeau et al. 2001; Herzog et al. 2001; Takamori et al. 2001; Kaneko and Fujiyama 2002; Härtig et al. 2003). One reason for this difference may be that the SOC nuclei receive a large number of converging afferents, from both the ascending and the descending pathways (Huffman and Henson 1990; Helfert et al. 1991; Spangler and Warr 1991). These inputs differ in functional aspects and may well express different VGLUT isoforms.

VGLUT1 and VGLUT2 are considered as reliable markers for glutamatergic synapses (Fremeau et al. 2001). Indeed, the distribution of VGLUT1-immunoreactive and VGLUT2-immunoreactive terminals in the adult SOC nuclei, as seen in the present study, is in agreement with the results of

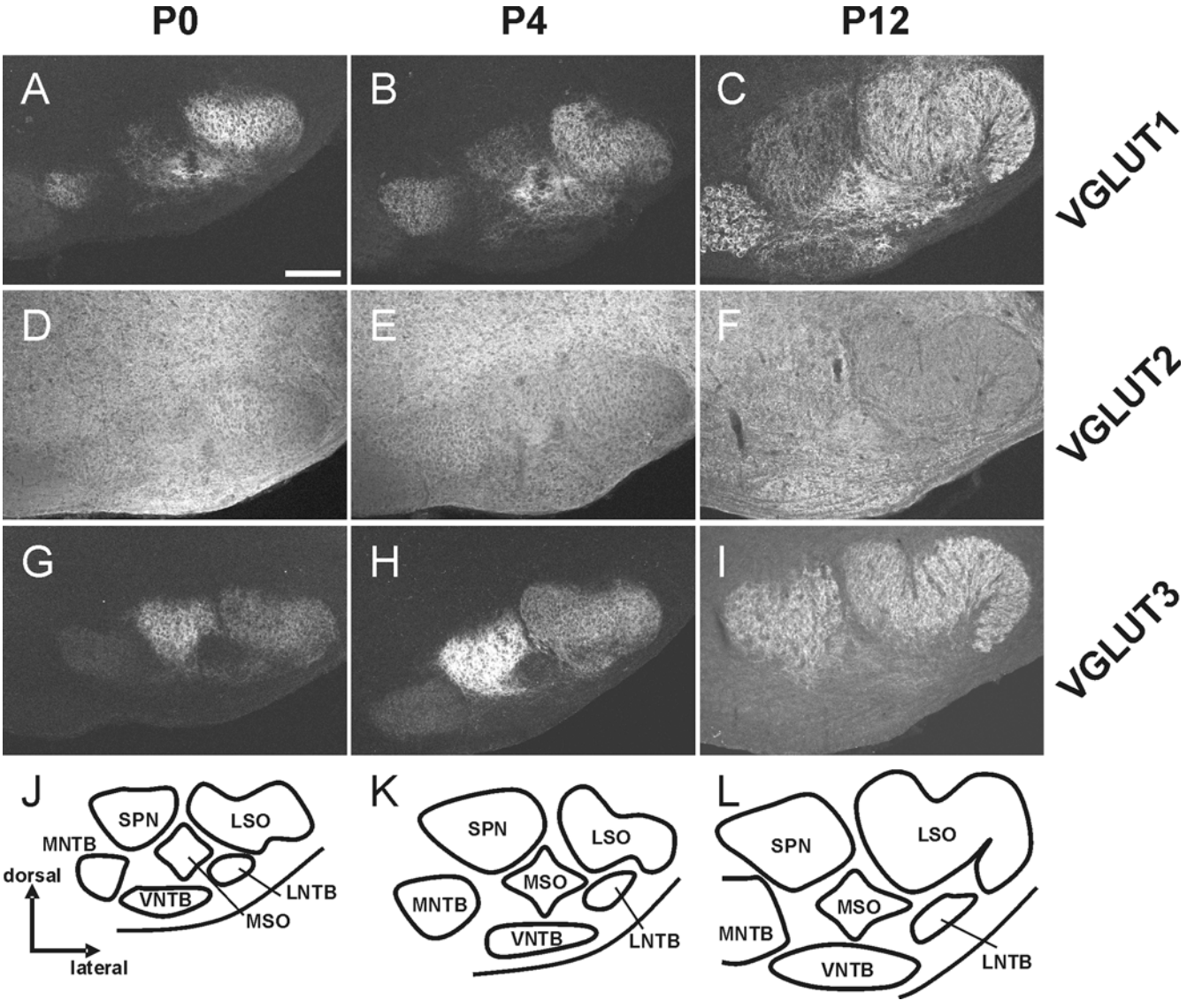

Fig. 3 **a–i** Overview of VGLUT-ir in the developing rat SOC between P0 and P12. **a–c** VGLUT1-ir is dense in the MNTB, the MSO, the LSO, and the LNTB at P0 and thereafter. Labeling is also clearly seen in the SPN at all ages but is weaker. Almost no VGLUT1-ir is present in the VNTB at P0 and P4, becoming weak by P12 (see also Fig. 5a–c). At all ages, brainstem areas outside the SOC are virtually unlabeled. **d–f** VGLUT2-ir in all six nuclei is moderate at all ages. **g–i** VGLUT3-ir at P0 and P4 is highest in the SPN. Labeling in the LSO is also obvious at all ages and increases with age. Aside from LSO and SPN, only the neonatal MNTB and LNTB (P0 and P4) show some VGLUT3-ir at this low magnification. By P12, moderate labeling is visible in the MSO and faint labeling in the VNTB. **j–l** Semi-schematic representations of the developing rat SOC, illustrating the localization and borders of the six nuclei. *Bar* 200 μm

previous papers describing glutamatergic inputs into the SOC. Such glutamatergic inputs are best characterized in the MNTB, LSO, and MSO (for reviews, see Caspary and Finlayson 1991; Helfert et al. 1991; Yin 2002; for a recent summary of the literature, see Srinivasan et al. 2004). Our data not only confirm the general distribution pattern of glutamatergic inputs into these nuclei, but are also in accordance with results of the cellular distribution. First, the thick fenestrated labeling pattern that we saw for both transporters in the MNTB is consistent with previous results (Varoqui et al. 2002) and strikingly similar to the pattern seen for calyces of Held with intracellular dye labeling techniques (Friauf and Ostwald 1988; Forsythe 1994; von Gersdorff and Borst 2002). These specialized synaptic terminals are known to be glutamatergic (Grandes and Streit 1997). Second, in the MSO, the localization of the transporters in the neuropil, rather than on the somata, is in accordance with the termination pattern of the afferent axons that originate from the cochlear nuclear complex and that are presumed to be glutamatergic (Kiss and Majorossy 1983; Suneja et al. 1995). Finally, our data of VGLUT distribution in the neuropil of the LSO are in line with previous findings (Caicedo and Eybalin 1999; Liu 2003). Taken together, as in other brain areas, VGLUT-immunoreactive terminals appear to identify glutamatergic synapses in the SOC.

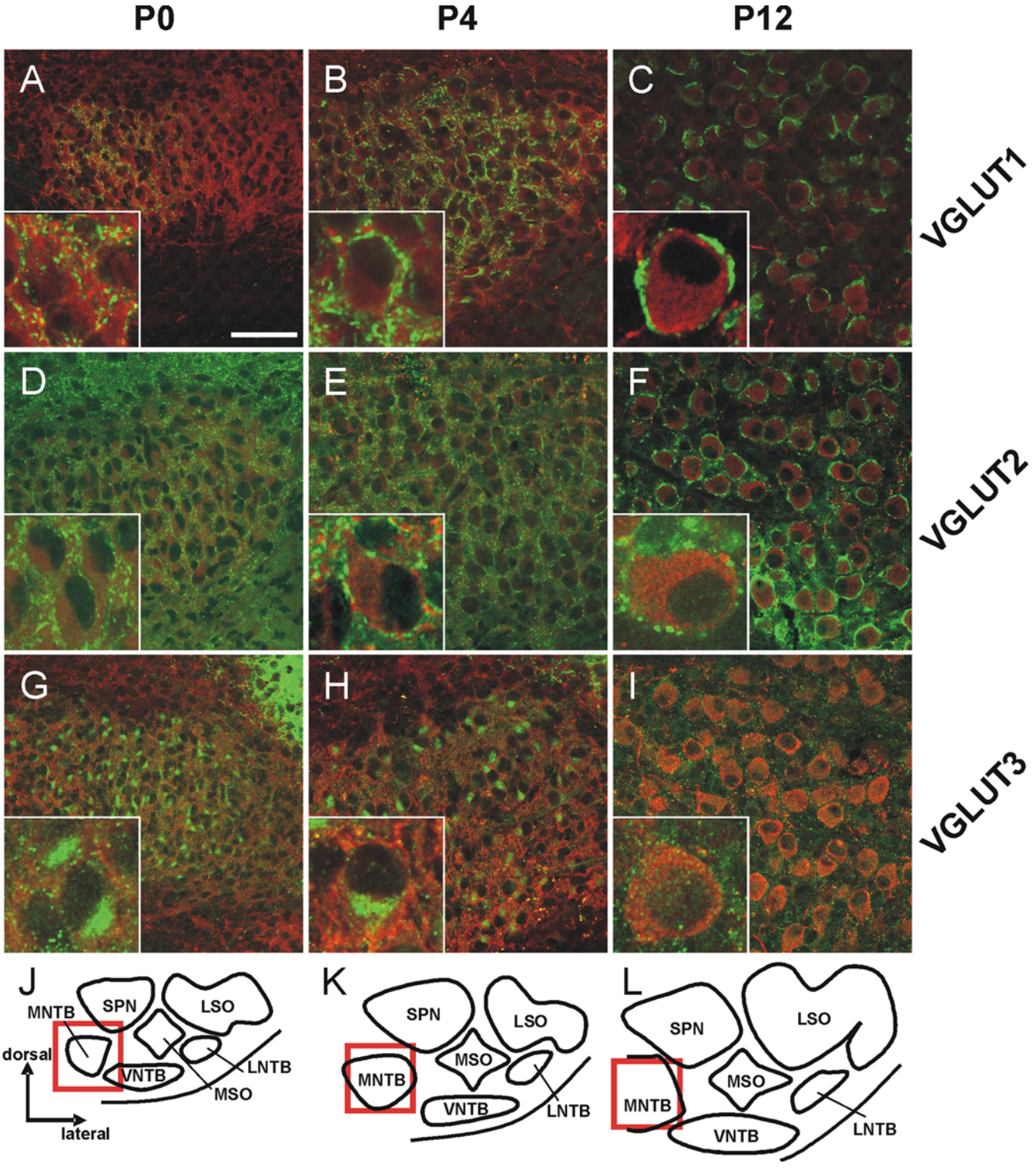

Fig. 4 **a–i** High magnification confocal images illustrating VGLUT-ir in the developing MNTB. VGLUT-ir is *green*, and MAP2-ir is *red*. **a–c** VGLUT1-ir changes from a punctate pattern in the neuropil at P0 to a thick fenestrated labeling pattern around the somata of MNTB principal neurons at P12; an intermediate pattern is present at P4. Cytoplasmic labeling of MNTB somata is never observed with VGLUT1 (*insets*). **d–f** VGLUT2-ir develops in a similar fashion to that seen with VGLUT1. **g–i** VGLUT3-ir displays an interesting feature with strong cytoplasmic signalling in MNTB somata at P0 and P4. This pattern is not obvious at P12 and thereafter, when immunoreactive grains are diffusely spread over the cytoplasm. **j–l** Semi-schematic representations of the rat SOC, illustrating the six nuclei (*red squares* localization of the high power photomicrographs). *Bar* 50 μm (*insets* 12.5 μm)

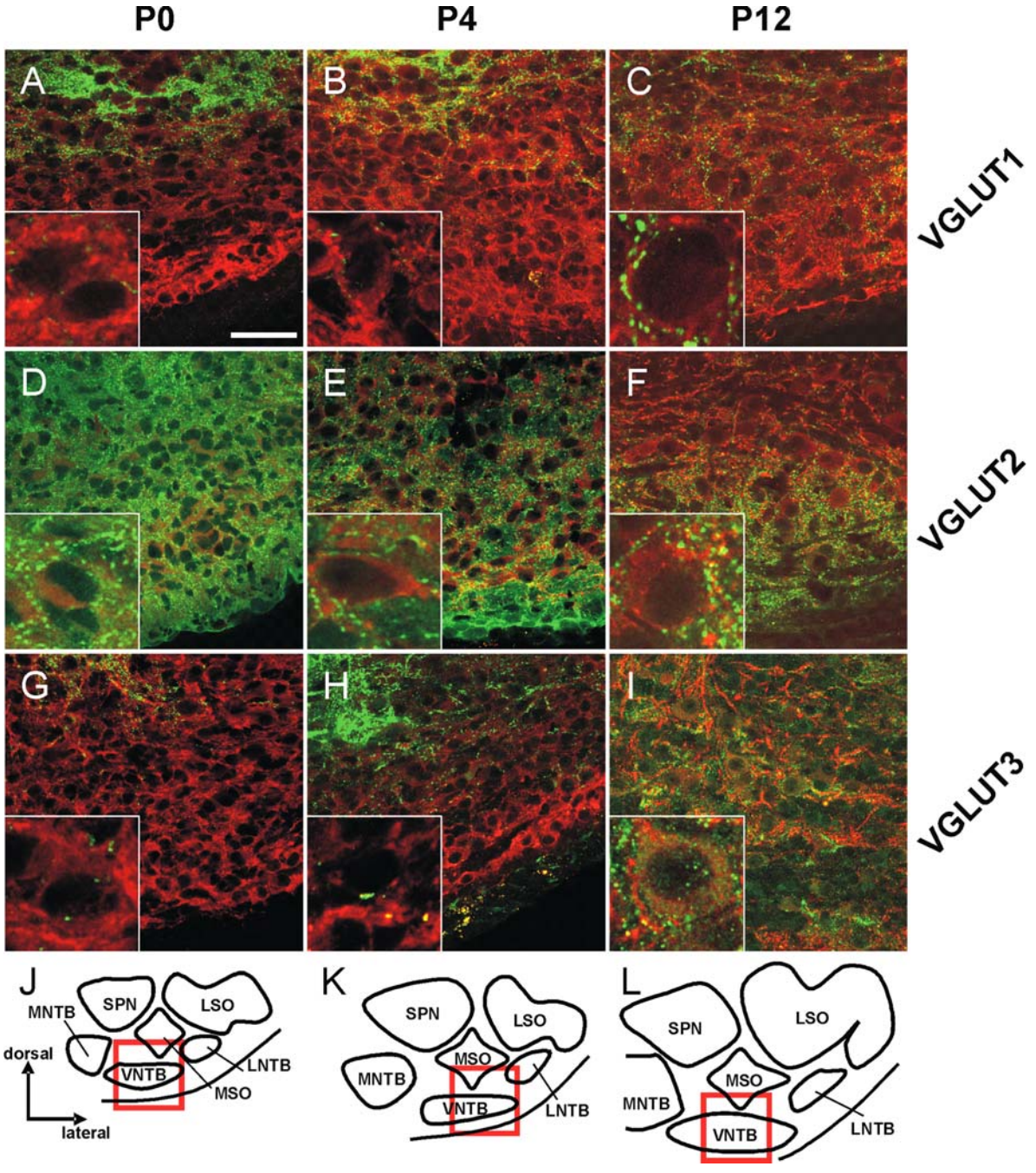

Fig. 5 **a–i** High magnification confocal images illustrating VGLUT-ir in the developing VNTB. VGLUT-ir is *green*, and MAP2-ir is *red*. **a–c** VGLUT1-ir is almost absent at P0 and P4. The number of puncta increases until P12, reaching an adult-like pattern at this age. **d–f** VGLUT2-ir is moderate throughout development. Puncta around the somata (*insets*) and in the neuropil are present at all ages and appear to be equally distributed. **g–i** VGLUT3-ir is almost absent at P0 and P4. A grainy diffuse labeling pattern in the neuropil can be observed at P12. **j–l** Semi-schematic representations of the rat SOC, illustrating the six nuclei (*red squares* localization of the high power photomicrographs). *Bar* 50 μm (*insets* 12.5 μm)

Less is known about the glutamatergic innervation of the VNTB, LNTB, and SPN (Smith and Spirou 2002). Glutamatergic input to VNTB neurons has been described physiologically (Robertson 1996) and by gross immunohistochemistry (Caicedo and Eybalin 1999). Our paper is the first to describe presumed glutamatergic terminals at the cellular level in the VNTB. In the LNTB, we have found disc-shaped terminals on the somata by both VGLUT1 and VGLUT2 immunohistochemistry. These disc-shaped terminals are reminiscent of the large endbulb-like nerve terminals onto LNTB neurons described earlier and thought to represent excitatory inputs originating from the ventral cochlear nucleus (Spirou et al. 1998). Our data provide strong evidence for the glutamatergic nature of these inputs and for the co-expression of two isoforms of VGLUT. In the SPN, we have observed only a small number of VGLUT-

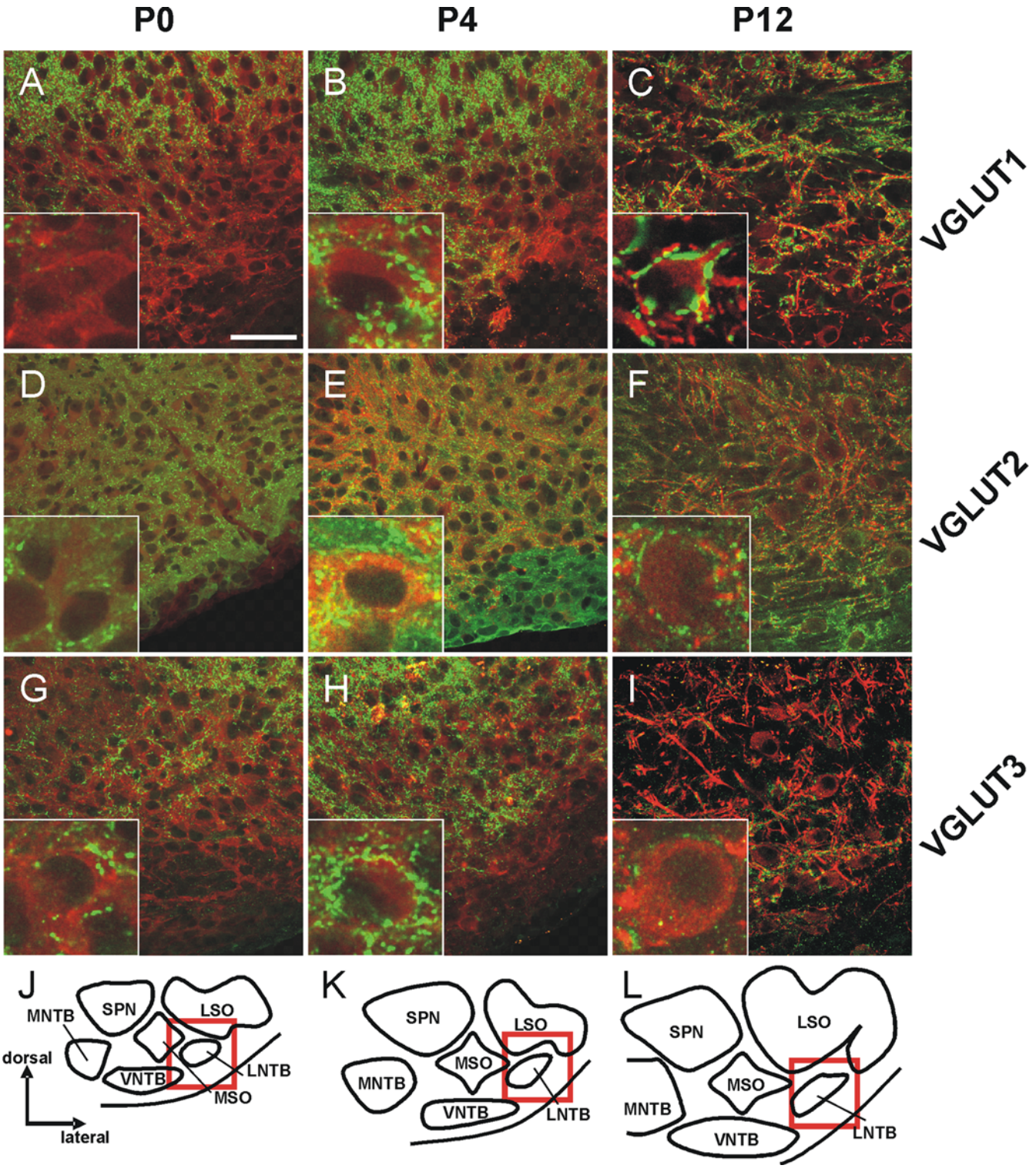

Fig. 6 **a–i** High magnification confocal images illustrating VGLUT-ir in the developing LNTB. VGLUT-ir is *green*, and MAP2-ir is *red*. **a–c** The number of VGLUT1-ir puncta is low at P0 and increases until P4. This pattern remains. **d–f** By birth, VGLUT2-ir can be seen both around the somata and in the neuropil in which it is equally distributed. The disc-shaped perisomatic labeling pattern and the faint cytoplasmic signal seen at P60 (Fig. 1f) have not arisen by P12. **g–i** At all ages, VGLUT3-ir has a punctate pattern and is present in the neuropil and around somata. Interestingly, the signal intensity appears to be highest at P4. **j–l** Semi-schematic representations of the rat SOC, illustrating the six nuclei (*red squares* localization of the high power photomicrographs). *Bar* 50 μm (*insets* 12.5 μm)

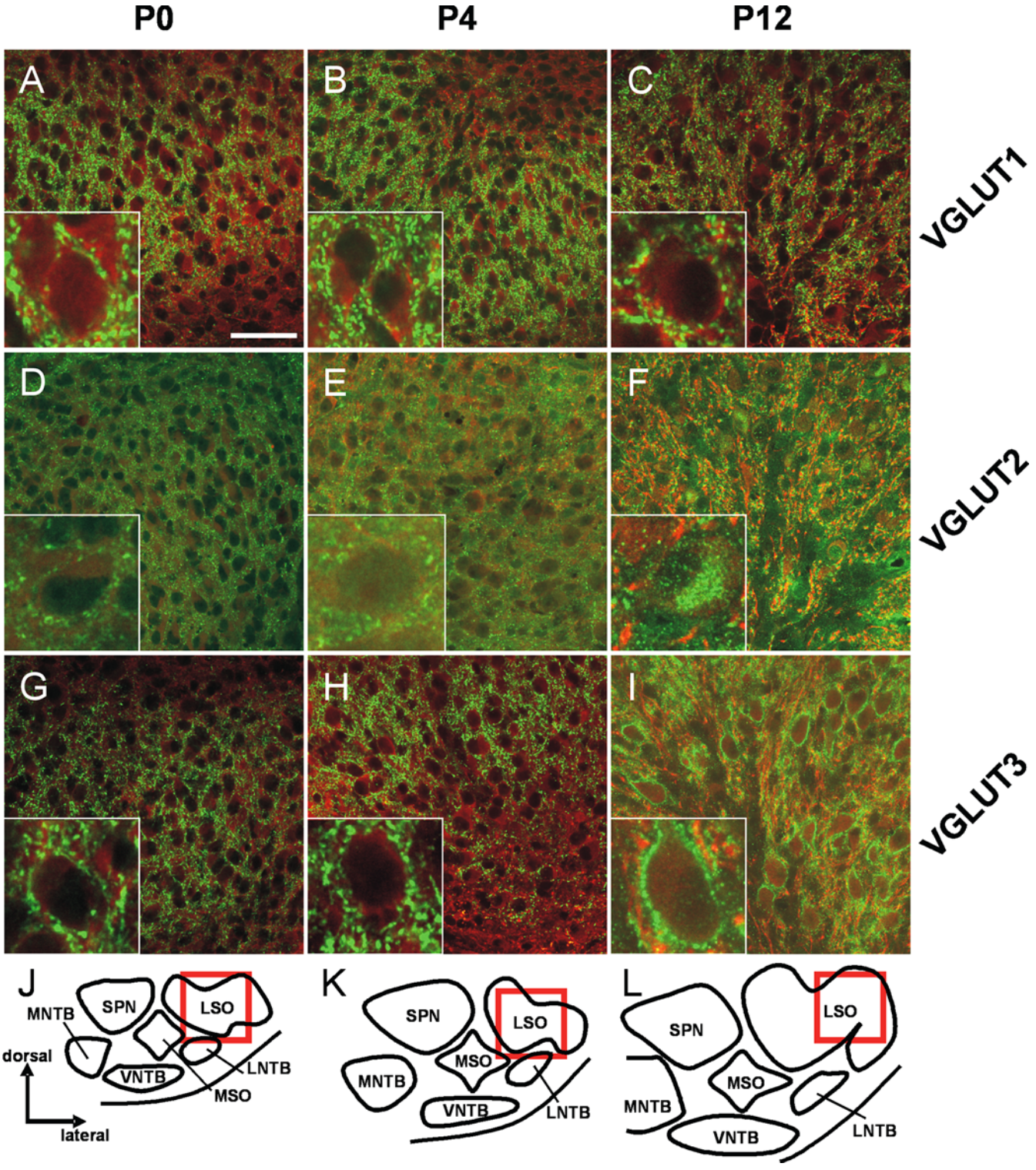

Fig. 7 **a–i** High magnification confocal images illustrating VGLUT-ir in the developing LSO. VGLUT-ir is *green*, and MAP2-ir is *red*. **a-c** At all ages, a punctate VGLUT1-ir is observed with no notable change in intensity. In contrast to P60 (cf. Fig. 2a), immunoreactive puncta are located both perisomatically and in the neuropil between P0 and P12. **d–f** VGLUT2-ir is also punctate and appears equally distributed in the neuropil and around somata. This pattern is present from P0 to P12. Cytoplasmic staining is observed at P12 and resembles that at P60 (cf. Fig. 2d). **g–i** VGLUT3-ir puncta decorate somata at all ages. Their density increases with age, becoming particularly high at P12, when somata and proximal dendrites are clearly outlined and decorated (*insets*). Aside from a perisomatic distribution, immunoreactive puncta also occur in the neuropil. **j–l** Semi-schematic representation of the rat SOC, illustrating the six nuclei (*red squares* localization of the high power photomicrographs). *Bar*: 50 μm (*insets* 12.5 μm)

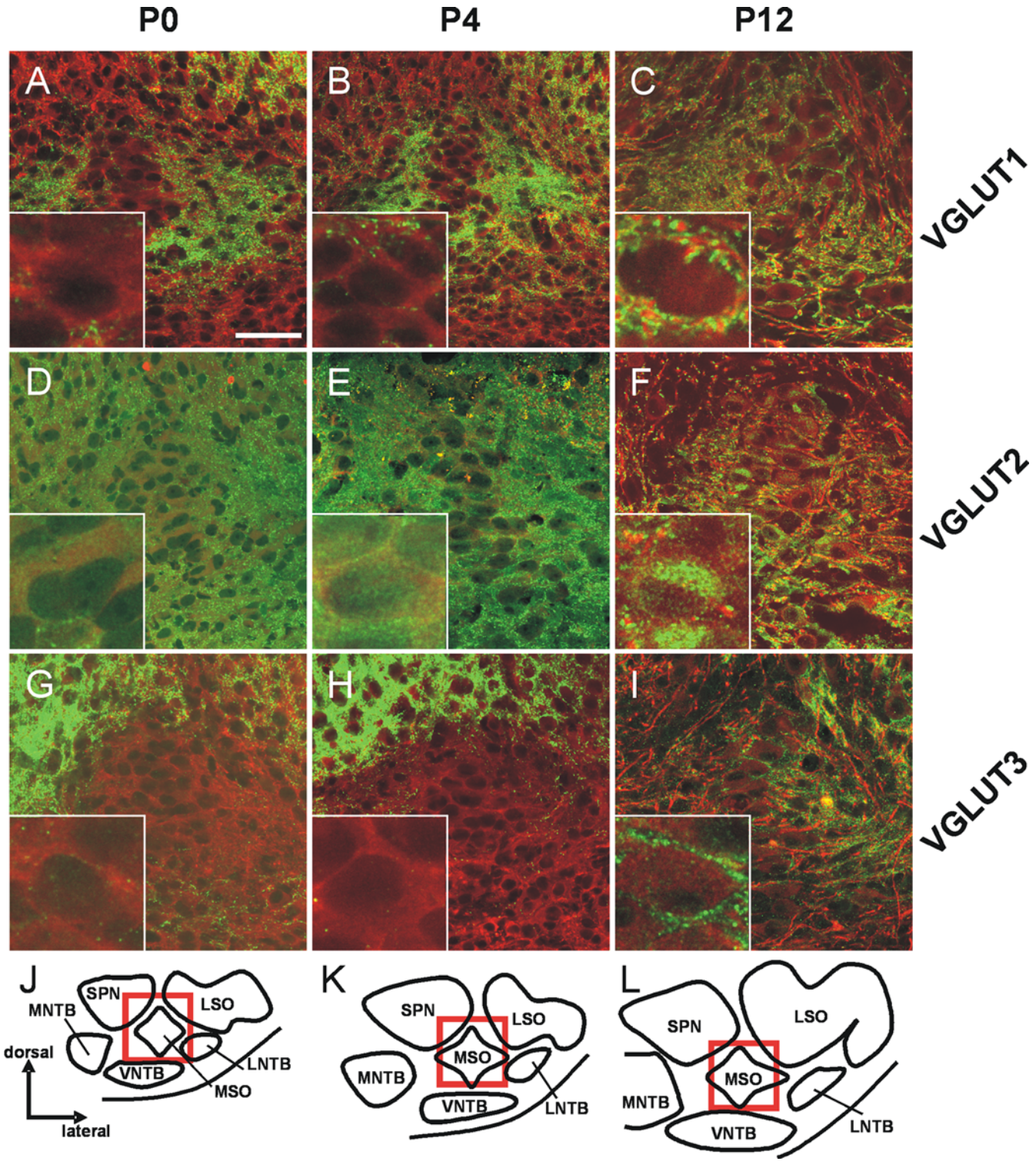

Fig. 8 **a–i** High magnification confocal images illustrating VGLUT-ir in the developing MSO. VGLUT-ir is *green*, and MAP2-ir is *red*. **a–c** VGLUT1-ir is strong at all ages. A striking observation is the location of the puncta, which appear to lie medial and lateral to the somata column, i.e., in the dendritic region. In addition to the neuropil labeling, a perisomatic distribution becomes clear only at P12. **d–f** VGLUT2-ir is present at all ages. The labeling pattern is diffuse and dense in the neuropil in which grains are equally spread. Perisomatic puncta are rare. Moderate cytoplasmic labeling is observed at P12. **g–i** VGLUT3-ir is virtually absent at P0 and P4 but can be seen as a punctate pattern at P12. Immunoreactive puncta occur around somata and in the neuropil. **j–l** Semi-schematic representations of the rat SOC, illustrating the six nuclei (*red squares* localization of the high power photomicrographs). *Bar* 50 μm (*insets* 12.5 μm)

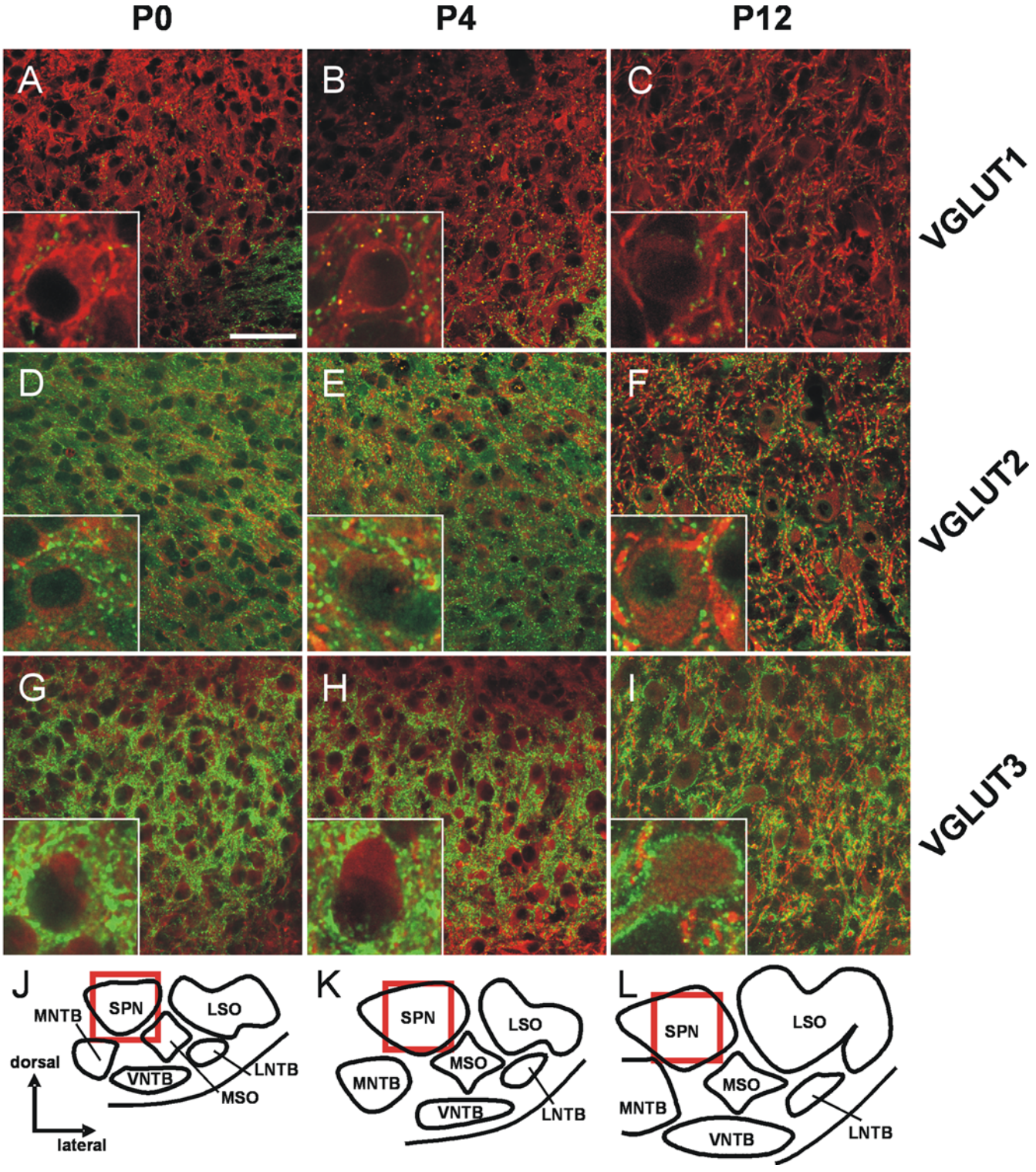

Fig. 9 **a–i** High magnification confocal images illustrating VGLUT-ir in the developing SPN. VGLUT-ir is *green*, and MAP2-ir is *red*. **a–c** Throughout postnatal development, VGLUT1-ir is restricted to a few puncta in the neuropil. Note dorsal aspects of MSO displaying immunolabel at *lower right* in **a, b** (see also Figs. 3a, b, 8a, b). **d–f** VGLUT2-ir has a punctate appearance at all ages and is equally distributed across the nucleus. Cytoplasmic labeling, as seen in adults (cf. Fig. 2f), is not visible between P0 and P12. **g–i** VGLUT3-ir is intense from P0 until P12. A perisomatic and neuropil labeling pattern is present at all ages, whereas proximal dendrites do not become outlined prior to P4. The soma-dendritic labeling pattern becomes more prominent at P12 and resembles that in the LSO at this age (cf. Fig. 7i) with clear differences from the adult appearance (cf. Fig. 2i). **j–l** Semi-schematic representation of the rat SOC, illustrating the six nuclei (*red squares* localization of the high power photomicrographs) *Bar* 50 μm (*insets* 12.5 μm)

immunoreactive terminals, predominantly in the neuropil. Many, but not all, SPN neurons are excited upon acoustic stimulation (Behrend et al. 2002; Dehmel et al. 2002; Kulesza et al. 2003), and octopus and multipolar cells in the contralateral ventral cochlear nucleus project into the SPN (Friauf and Ostwald 1988; Schofield 1995). Schofield (1995) has described two types of terminals ending on the somata. This pattern is in contrast to our observation. At present, the reasons for the different results are unclear.

Neurons in several SOC nuclei display cytoplasmic VGLUT labeling (LSO, SPN, LNTB for VGLUT2; MNTB for VGLUT3). This is indicative of a glutamatergic phenotype of these neurons. Support for this conclusion is provided in the retina in which some bipolar cells and ganglion cells have been described as being VGLUT1- and VGLUT2-immunoreactive, respectively (Fyk-Kolodziej et al. 2004). Both types of retinal neurons are known to be glutamatergic. Nevertheless, there is no strict correlation between the presence of VGLUT-ir in the soma and a glutamatergic phenotype, e.g., cortical pyramidal cells (also known to be glutamatergic), have been shown to be VGLUT1- and VGLUT2-immunonegative (Varoqui et al. 2002). Thus, some of the SOC neurons, whose somata have remained unlabeled in the present study, might nevertheless use glutamate as their transmitter. The presence of VGLUT2 in LSO somata implies that a considerable subpopulation of rat LSO neurons is glutamatergic. Indeed, about 50% of the cells within the cat LSO have been shown to be glutamate-immunoreactive (Glendenning et al. 1992). A similarly high number is suggested by our data. We have also found VGLUT2 signals in the somata of many SPN neurons. Although SPN neurons are generally considered to be GABAergic (Kulesza and Berrebi 2000) and LNTB neurons to be GABAergic and glycinergic (Helfert et al. 1989; Spirou and Berrebi 1997), the present results for somatic VGLUT2-ir suggest that a few of them may be glutamatergic. Finally, the VGLUT3-ir that we have observed in almost all MNTB somata indicates the glutamatergic phenotype of these neurons. This is surprising if one considers the glycinergic character of MNTB neurons (Helfert et al. 1989; Friauf et al. 1999). However, VGLUT3 is not a marker for conventional glutamatergic neurons and coexpression in glycinergic neurons has also been described in the retina (Haverkamp and Wässle 2004). An unsuspected neuromodulatory function of VGLUT3 has been proposed in agreement with this (Herzog et al. 2004).

Developmental changes in VGLUT immunoreactivity

Our results demonstrate changes of VGLUT expression at several levels in the SOC. Changes in the intensity of the immunoreactive signal occur with VGLUT1 and VGLUT3, whereas VGLUT2-ir remains moderate throughout development. VGLUT1-ir increases from a virtual absence at P0 and P4 in terminals in the VNTB to the adult-like pattern at P12. A similar increase has been observed in the LNTB, except that the adult-like pattern is achieved as early as P4. Like VGLUT1, VGLUT3-ir is almost absent in the VNTB of neonatal animals but is present at P12 and thereafter. Together, these results imply a progressive development of VGLUT1 and VGLUT3 expression in some SOC nuclei. Aside from progressive processes, we have also observed regressive processes. One example of regressive development is provided by the MNTB in which the neuronal cytoplasm strongly labels for VGLUT3 until P4 but has a weak pattern thereafter. Another example is VGLUT3-ir in the LNTB; this labeling is highest during the first postnatal week (P0, P4) and declines with increasing age (P12, P60). Interestingly, changes in VGLUT-ir are also characterized by a combination of progressive and regressive processes. Such a transient feature is seen in the LSO and the MSO in which VGLUT3 is up-regulated between P0–P12 and P4–P12, respectively. By P60, the immunoreactive signal has declined in both nuclei. Our results therefore suggest that VGLUT1 is up-regulated in the VNTB and LNTB and constantly expressed in the MNTB, LSO, and MSO (with almost no expression in the SPN). VGLUT2 does not appear to be dynamically regulated with age. VGLUT3-ir shows all three types of age-related changes; a progressive course in the VNTB, a regressive course in the MNTB, SPN, and LNTB, and a combination of both in the LSO and MSO. The age-dependent up-regulation of VGLUT1 is in accordance with previous findings in other brain regions (Ni et al. 1995; Schäfer et al. 2002; Miyazaki et al. 2003), whereas the constant expression levels of VGLUT2 contrast with the observation that this transporter isoform is down-regulated with age (Miyazaki et al. 2003). As data on VGLUT3 development are not available from other studies, our data reveal, for the first time, that this transporter can have a diverse time course across various nuclei.

Another developmental aspect that is worthwhile considering is the dynamics in the distribution pattern of the VGLUT-ir. We have observed age-related changes in the localization of immunoreactive puncta in the LSO and MSO (VGLUT1 and VGLUT3) and in the SPN (VGLUT3). These changes are characterized by strong transient perisomatic labeling (most obvious at P12) that disappears by P60. None of the three isoforms displays any perisomatic labeling in the adult LSO and SPN, and only a weak VGLUT3-ir remains on MSO somata. This is indicative of a withdrawal and subsequent elimination of glutamatergic synapses from the neuronal somata in these nuclei. As the disappearance of perisomatic immunoreactivity occurs after P12, i.e., after the onset of hearing (Geal-Dor et al. 1993), the acoustically evoked activity presumably plays a role in reorganization processes. Analysis of VGLUT-ir in deaf or hearing-impaired mice should therefore be interesting. Experience-dependent reorganizations, requiring proper acoustic input, have recently been described for inhibitory glycinergic inputs on MSO neurons of gerbils (Kapfer et al. 2002). In contrast to our results, however, these changes are seen as a spatial refinement of synapses during development, starting from a diffuse distribution along the somata and dendrites in juveniles and ending up by being confined to the somata and the most proximal dendrites. Thus, glycinergic and glutamatergic synapses to MSO neurons undergo a reciprocal pattern of development, in that glycinergic inputs are re-

organized in a centripetal manner, whereas glutamatergic inputs display centrifugal changes. The developmental changes of VGLUT1-ir and VGLUT2-ir in the MNTB correlate nicely with the age-related changes reported for calyces of Held. The maturation of the calyx is characterized by gross morphological changes during the first two postnatal weeks (Morest 1968; Kandler and Friauf 1993). Consistent with these observations, the calyx-like labeling pattern of VGLUTs seen in adulthood is not present before P12. These results provide further evidence that VGLUT-ir can be used to describe changes in glutamatergic synapses.

Functional significance of VGLUT expression

Consistent with their high sequence homology, the three VGLUT isoforms are highly similar with respect to substrate specificity, kinetics, and pharmacology (for a summary of the literature, see Wojcik et al. 2004). With respect to possible functional differences, VGLUT1 has been postulated to be present in terminals of highly plastic synapses, whereas VGLUT2 has been suggested to occur in terminals with a high release probability (Liu 2003). Our data from MNTB synapses, implying a co-distribution in the calyces of Held, are in accordance, because these synapses are able to transmit signals with high fidelity (Trussell 1999) and display short-term plasticity (von Gersdorff et al. 1997; von Gersdorff and Borst 2002). The MNTB synapses are a useful model for untangling the two functional aspects, and animals that are deficient for one or other isoform should enable a direct analysis. Thus far, VGLUT1 −/− mice have been generated (Fremeau et al. 2004a; Wojcik et al. 2004).

The transiently high expression of VGLUT1 (on MSO and LSO somata) and VGLUT3 (in MSO, LSO, and SPN) is suggestive of a developmental role of the two isoforms. As VGLUT3 expression becomes weaker until adulthood, we conclude that the role of this transporter is basically restricted to early developmental aspects, such as synapse maturation. By contrast, VGLUT1, which remains highly expressed until P60, is concluded to play a role both during maturation and in adulthood. A developmentally restricted role of VGLUT1 is likely to exist during the temporally restricted innervation period of MSO and LSO somata by glutamatergic terminals. Finally, the role of VGLUT2 appears to be similar throughout life in the SOC, as changes in the intensity and distribution pattern are not obvious.

A specific developmental role of VGLUT3 is indicated by our results showing cytoplasmic labeling in the MNTB and the concomitant labeling of synaptic terminals in the LSO, MSO, and SPN. All these regions are target nuclei of MNTB neurons (Sommer et al. 1993). Interestingly, these MNTB neurons are glycinergic in the adult and both GABAergic and glycinergic during the first 2–3 weeks in some rodent species (Kotak et al. 1998; Kullmann et al. 2002). Thus, VGLUT3 is evidently involved in the maturation processes of a glycinergic projection. A striking implication of this is that the three transmitters may be co-released from MNTB axon terminals. Indeed, such a co-release has been reported recently (Kandler and Gillespie 2004).

The characterization of the phenotype of VGLUT1-deficient mice has demonstrated that the animals exhibit no gross abnormalities for about 2 weeks after birth, but they die between P18 and P21, unless specific care is provided (Fremeau et al. 2004a; Wojcik et al. 2004). Thus, VGLUT1 expression becomes essential for survival at the time of the developmental switch from VGLUT2 to VGLUT1 in the CNS (Miyazaki et al. 2003). Because of the profound effects following VGLUT1 deficiency, and since our data show VGLUT1 strong expression in the SOC during the first two postnatal weeks, we hypothesize that the sound localization circuits, in which the SOC nuclei play a crucial role, are massively disturbed in VGLUT1 −/− mice. Several important aspects of circuitry development in the SOC have been well documented as taking place during the transiently high expression of VGLUT1, both in the excitatory glutamatergic and in the inhibitory glycinergic inputs (Sanes and Siverls 1991; Kotak and Sanes 1997; Rietzel and Friauf 1998; Kapfer et al. 2002; Kim and Kandler 2003).

Acknowledgements We thank Dr. S. El Mestikawy for the generous gift of the VGLUT antibodies and Dr. J.W. Deitmer and G. Neumann for help with the confocal microscope.

References

Aihara Y, Mashima H, Onda H, Hisano S, Kasuya H, Hori T, Yamada S, Tomura H, Yamada Y, Inoue I, Kojima I, Takeda J (2000) Molecular cloning of a novel brain-type Na^+-dependent inorganic phosphate cotransporter. J Neurochem 74:2622–2625

Behrend O, Brand A, Kapfer C, Grothe B (2002) Auditory response properties in the superior paraolivary nucleus of the gerbil. J Neurophysiol 87:2915–2928

Bellocchio EE, Reimer RJ, Fremeau RT, Edwards RH (2000) Uptake of glutamate into synaptic vesicles by an inorganic phosphate transporter. Science 289:957–960

Brew HM, Forsythe ID (1995) Two voltage-dependent K^+ conductances with complementary functions in postsynaptic integration at a central auditory synapse. J Neurosci 15:8011–8022

Caicedo A, Eybalin M (1999) Glutamate receptor phenotypes in the auditory brainstem and mid-brain of the developing rat. Eur J Neurosci 11:51–74

Caspary DM, Finlayson PG (1991) Superior olivary complex: functional neuropharmacology of the principal cell types. In: Altschuler RA, Bobbin RP, Clopton BM, Hoffman DW (eds) Neurobiology of hearing: the central auditory system. Raven, New York, pp 141–161

Dehmel S, Kopp-Scheinpflug C, Dörrscheidt GJ, Rübsamen R (2002) Electrophysiological characterization of the superior paraolivary nucleus in the Mongolian gerbil. Hearing Res 172:18–36

Dingledine R, Borges K, Bowie D, Traynelis SF (1999) The glutamate receptor ion channels. Pharmacol Rev 51:7–61

Dodson PD, Forsythe ID (2004) Presynaptic K^+ channels: electrifying regulators of synaptic terminal excitability. Trends Neurosci 27:210–217

Forsythe ID (1994) Direct patch recording from identified presynaptic terminals mediating glutamatergic EPSCs in the rat CNS, in vitro. J Physiol (Lond) 479:381–387

Fremeau RT, Troyer MD, Pahner I, Nygaard GO, Tran CH, Reimer RJ, Bellocchio EE, Fortin D, Storm-Mathisen J, Edwards RH (2001) The expression of vesicular glutamate transporters defines two classes of excitatory synapse. Neuron 31:247–260

Fremeau RT, Burman J, Qureshi T, Tran CH, Proctor J, Johnson J, Zhang H, Sulzer D, Copenhagen DR, Storm-Mathisen J, Reimer RJ, Chaudhry FA, Edwards RH (2002) The identification of vesicular glutamate transporter 3 suggests novel modes of signaling by glutamate. Proc Natl Acad Sci USA 99:14488–14493

Fremeau RT, Kam K, Qureshi T, Johnson J, Copenhagen DR, Storm-Mathisen J, Chaudhry FA, Nicoll RA, Edwards RH (2004a) Vesicular glutamate transporters 1 and 2 target to functionally distinct synaptic release sites. Science 304:1815–1819

Fremeau RT, Voglmaier S, Seal RP, Edwards RH (2004b) VGLUTs define subsets of excitatory neurons and suggest novel roles for glutamate. Trends Neurosci 27:98–103

Friauf E, Ostwald J (1988) Divergent projections of physiologically characterized rat ventral cochlear nucleus neurons as shown by intraaxonal injection of horseradish peroxidase. Exp Brain Res 73:263–284

Friauf E, Aragón C, Löhrke S, Westenfelder B, Zafra F (1999) Developmental expression of the glycine transporter GLYT2 in the auditory system of rats suggests involvement in synapse maturation. J Comp Neurol 412:17–37

Fyk-Kolodziej B, Dzhagaryan A, Qin P, Pourcho RG (2004) Immunocytochemical localization of three vesicular glutamate transporters in the cat retina. J Comp Neurol 475:518–530

Geal-Dor M, Freeman S, Li G, Sohmer H (1993) Development of hearing in neonatal rats: air and bone conducted ABR thresholds. Hearing Res 69:236–242

Gersdorff H von, Borst JGG (2002) Short-term plasticity at the calyx of Held. Nat Rev Neurosci 3:53–64

Gersdorff H von, Schneggenburger R, Weis S, Neher E (1997) Presynaptic depression at a calyx synapse: the small contribution of metabotropic glutamate receptors. J Neurosci 17:8137–8146

Glendenning KK, Baker BN, Hutson KA, Masterton RB (1992) Acoustic chiasm V: inhibition and excitation in the ipsilateral and contralateral projections of LSO. J Comp Neurol 319:100–122

Grandes P, Streit P (1997) Glutamate-like immunoreactivity in calyces of Held. J Neurocytol 18:685–693

Gras C, Herzog E, Bellenchi GC, Bernard V, Ravassard P, Pohl M, Gasnier B, Giros B, El Mestikawy S (2002) A third vesicular glutamate transporter expressed by cholinergic and serotoninergic neurons. J Neurosci 22:5442–5451

Härtig W, Riedel A, Grosche J, Edwards RH, Fremeau RT, Harkany T, Brauer K, Arendt T (2003) Complementary distribution of vesicular glutamate transporters 1 and 2 in the nucleus accumbens of rat: relationship to calretinin-containing extrinsic innervation and calbindin-immunoreactive neurons. J Comp Neurol 465:1–10

Haverkamp S, Wässle H (2004) Characterization of an amacrine cell type of the mammalian retina immunoreactive for vesicular glutamate transporter 3. J Comp Neurol 468:251–263

Helfert RH, Bonneau JM, Wenthold RJ, Altschuler RA (1989) GABA and glycine immunoreactivity in the guinea pig superior olivary complex. Brain Res 501:269–286

Helfert RH, Snead CR, Altschuler RA (1991) The ascending auditory pathways. In: Altschuler RA (ed) Neurobiology of hearing: the central auditory system. Raven, New York, pp 1–25

Herzog E, Bellenchi GC, Gras C, Bernard V, Ravassard P, Bedet C, Gasnier B, Giros B, El Mestikawy S (2001) The existence of a second vesicular glutamate transporter specifies subpopulations of glutamatergic neurons. J Neurosci 21:RC181

Herzog E, Gilchrist J, Gras C, Muzerelle A, Ravassard P, Giros B, Gaspar P, El Mestikawy S (2004) Localization of VGLUT3, the vesicular glutamate transporter type 3, in the rat brain. Neuroscience 123:983–1002

Hisano S (2003) Vesicular glutamate transporters in the brain. Anat Sci Int 78:191–204

Hisano S, Hoshi K, Ikeda Y, Maruyama D, Kanemoto M, Ichijo H, Kojima I, Takeda J, Nogami H (2000) Regional expression of a gene encoding a neuron-specific Na^+-dependent inorganic phosphate cotransporter (DNPI) in the rat forebrain. Mol Brain Res 83:34–43

Huffman RF, Henson OW (1990) The descending auditory pathway and acousticomotor systems: connections with the inferior colliculus. Brain Res Rev 15:295–323

Kandler K, Friauf E (1993) Pre- and postnatal development of efferent connections of the cochlear nucleus in the rat. J Comp Neurol 328:161–184

Kandler K, Gillespie DC (2004) Glutamatergic synaptic transmission in the developing GABA/glycinergic MNTB-LSO pathway. Third Symposium on Molecular Mechanisms in Central Auditory Function, Plasticity and Disorders. Jackson Hole, Wyoming, June 25–27th 2004

Kaneko T, Fujiyama F (2002) Complementary distribution of vesicular glutamate transporters in the central nervous system. Neurosci Res 42:243–250

Kaneko T, Fujiyama F, Hioki H (2002) Immunohistochemical localization of candidates for vesicular glutamate transporters in the rat brain. J Comp Neurol 444:39–62

Kapfer C, Seidl AH, Schweizer H, Grothe B (2002) Experience-dependent refinement of inhibitory inputs to auditory coincidence-detector neurons. Nat Neurosci 5:247–253

Kim G, Kandler K (2003) Elimination and strengthening of glycinergic/GABAergic connections during tonotopic map formation. Nat Neurosci 6:282–290

Kiss A, Majorossy K (1983) Neuron morphology and synaptic architecture in the medial superior olivary nucleus. Light- and electron-microscopic studies in the cat. Exp Brain Res 52:315–327

Kotak VC, Sanes DH (1997) Deafferentation weakens excitatory synapses in the developing central auditory system. Eur J Neurosci 9:2340–2347

Kotak VC, Korada S, Schwartz IR, Sanes DH (1998) A developmental shift from GABAergic to glycinergic transmission in the central auditory system. J Neurosci 18:4646–4655

Kulesza RJ, Berrebi AS (2000) Superior paraolivary nucleus of the rat is a GABAergic nucleus. J Assoc Res Otolaryngol 1:255–269

Kulesza RJ, Spirou GA, Berrebi AS (2003) Physiological response properties of neurons in the superior paraolivary nucleus of the rat. J Neurophysiol 89:2299–2312

Kullmann PHM, Ene FA, Kandler K (2002) Glycinergic and GABAergic calcium responses in the developing lateral superior olive. Eur J Neurosci 15:1093–1104

Liu GS (2003) Presynaptic control of quantal size: kinetic mechanisms for synaptic transmission and plasticity. Curr Opin Neurobiol 13:324–331

Löhrke S, Friauf E (2002) Developmental distribution of the glutamate receptor subunits KA2, GluR6/7, and delta 1/2 in the rat medial nucleus of the trapezoid body. A quantitative image analysis. Cell Tissue Res 308:19–33

Miyazaki T, Fukaya M, Shimizu H, Watanabe M (2003) Subtype switching of vesicular glutamate transporters at parallel fibre-Purkinje cell synapses in developing mouse cerebellum. Eur J Neurosci 17:2563–2572

Morest DK (1968) The growth of synaptic endings in the mammalian brain: a study of the calyces of the trapezoid body. Z Anat Entwickl-Gesch 127:201–220

Ni B, Rosteck PR Jr, Nadi NS, Paul SM (1994) Cloning and expression of a cDNA encoding a brain-specific Na^+ -dependent inorganic phosphate cotransporter. Proc Natl Acad Sci USA 91:5607–5611

Ni B, Wu X, Yan GM, Wang J, Paul SM (1995) Regional expression and cellular localization of the Na(+)-dependent inorganic phosphate cotransporter of rat brain. J Neurosci 15:5789–5799

Oertel D, Wickesberg RE (1993) Glycinergic inhibition in the cochlear nuclei: evidence for tuberculoventral neurons being glycinergic. In: Merchán MA, Juiz JM, Godfrey DA, Mugnaini E (eds) The mammalian cochlear nuclei: organization and function. Plenum, New York, London, pp 225–237

Raman IM, Zhang S, Trussell LO (1994) Pathway-specific variants of AMPA receptors and their contribution to neuronal signaling. J Neurosci 14:4998–5010

Rietzel H, Friauf E (1998) Neuron types in the rat lateral superior olive and developmental changes in the complexity of their dendritic arbors. J Comp Neurol 390:20–40

Robertson D (1996) Physiology and morphology of cells in the ventral nucleus of trapezoid body and rostral periolivary regions of the rat superior olivary complex studied in slices. Aud Neurosci 2:15–31

Sanes DH, Siverls V (1991) Development and specificity of inhibitory terminal arborizations in the central nervous system. J Neurobiol 8:837–854

Schäfer MKH, Varoqui H, Defamie N, Weihe E, Erickson JD (2002) Molecular cloning and functional identification of mouse vesicular glutamate transporter 3 and its expression in subsets of novel excitatory neurons. J Biol Chem 277:50734–50748

Schofield BR (1995) Projections from the cochlear nucleus to the superior paraolivary nucleus in guinea pigs. J Comp Neurol 360:135–149

Schwartz IR (1992) The superior olivary complex and lateral lemniscal nuclei. In: Webster DB, Popper AN, Fay RR (eds) The mammalian auditory pathway: neuroanatomy. Springer, Berlin Heidelberg New York, pp 117–167

Smith PH, Spirou GA (2002) From the cochlea to the cortex and back. In: Oertel D, Fay AN, Popper AN (eds) Integrative functions in the mammalian auditory pathway. Springer, Berlin Heidelberg New York, pp 6–71

Sommer I, Lingenhöhl K, Friauf E (1993) Principal cells of the rat medial nucleus of the trapezoid body: an intracellular in vivo study of their physiology and morphology. Exp Brain Res 95:223–239

Spangler KM, Warr WB (1991) The descending auditory system. In: Altschuler RA, Bobbin RP, Clopton BM, Hoffman DW (eds) Neurobiology of hearing: the central auditory system. Raven, New York, pp 27–45

Spirou GA, Berrebi AS (1997) Glycine immunoreactivity in the lateral nucleus of the trapezoid body of the cat. J Comp Neurol 383:473–488

Spirou GA, Rowland KC, Berrebi AS (1998) Ultrastructure of neurons and large synaptic terminals in the lateral nucleus of the trapezoid body of the cat. J Comp Neurol 398:257–272

Srinivasan G, Friauf E, Löhrke S (2004) Functional glutamatergic and glycinergic inputs to several superior olivary nuclei of the rat revealed by optical imaging. Neuroscience 128:617–634

Suneja SK, Benson CG, Gross J, Potashner SJ (1995) Evidence for glutamatergic projections from the cochlear nucleus to the superior olive and the ventral nucleus of the lateral lemniscus. J Neurochem 64:161–171

Takamori S, Rhee JS, Rosenmund C, Jahn R (2000) Identification of a vesicular glutamate transporter that defines a glutamatergic phenotype in neurons. Nature 407:189–194

Takamori S, Rhee JS, Rosenmund C, Jahn R (2001) Identification of differentiation-associated brain-specific phosphate transporter as a second vesicular glutamate transporter (VGLUT2). J Neurosci 21:RC182

Takamori S, Malherbe P, Broger C, Jahn R (2002) Molecular cloning and functional characterization of human vesicular glutamate transporter 3. EMBO Rep 3:798–803

Trussell LO (1999) Synaptic mechanisms for coding timing in auditory neurons. Annu Rev Physiol 61:477–496

Varoqui H, Schäfer MKH, Zhu HM, Weihe E, Erickson JD (2002) Identification of the differentiation-associated Na+/P-I transporter as a novel vesicular glutamate transporter expressed in a distinct set of glutamatergic synapses. J Neurosci 22:142–155

Vitten H, Reusch M, Friauf E, Löhrke S (2004) Expression of functional kainate and AMPA receptors in developing lateral superior olive neurons of the rat. J Neurobiol 59:272–288

Wojcik SM, Rhee JS, Herzog E, Sigler A, Jahn R, Takamori S, Brose N, Rosenmund C (2004) An essential role for vesicular glutamate transporter 1 (VGLUT1) in postnatal development and control of quantal size. Proc Natl Acad Sci USA 101:7158–7163

Wu SH, Kelly JB (1993) Response of neurons in the lateral superior olive and medial nucleus of the trapezoid body to repetitive stimulation: intracellular and extracellular recordings from mouse brain slice. Hearing Res 68:189–201

Yin TCT (2002) Neural mechanisms of encoding binaural localization cues in the auditory brainstem. In: Oertel D, Fay RR, Popper AA (eds) Integrative functions in the mammalian auditory pathway. Springer, Berlin Heidelberg New York, pp 99–159